

# CORRELATING MICRO/NANO STRUCTURE MORPHOLOGY TO HIGH-STRAIN RATE PERFORMANCE OF NANO-PARTICLE REINFORCED POLYMERIC MATERIALS

**M. IRSHIDAT, A. AL-OSTAZ, AND A.H.-D. CHENG**

Nano Infrastructure Research Group-Department of Civil Engineering  
University of Mississippi  
Oxford, Mississippi, 38677-1848, USA

## ABSTRACT

This paper focuses on correlating micro/nano structure morphology to performance of nano enhanced polymers subjected to blast loading, studying the behavior of these materials at high strain rates, and evaluating the effect of voids' size and amount on the strain rate sensitivity of nano materials. Three polyurea-based elastomeric materials are investigated in this study: unreinforced polyurea; Exfoliated Graphene Nano Particle (xGnP) reinforced polyurea; and Polyhedral Oligomeric Silsesquioxane (POSS) reinforced polyurea. 3D CT scan images show large amounts of randomly distributed voids in the materials. The study found that POSS reinforced polyurea has the largest number but the smallest void size among the three tested materials. Computational parametric evaluation is conducted to investigate the effect of such defects on the behavior of these materials. The results show that the rate dependence mechanism relies not only on the void ratio but also on void size.

*Key words: Nano, polymers, polyurea, strain rate, voids*

## 1. INTRODUCTION

A critical issue for the development of nanotechnology is the ability to understand, model, and simulate the behavior of small structures and to make the connection between nano structure properties and their macroscopic functions. Material modeling and simulation help in understanding the process, setting the objectives that could guide laboratory efforts, and controlling material structures, properties, and processes at physical implementation. These capabilities are vital to engineering design at the component and systems level (Cheng et al 2009).

Nanotechnology concepts make it possible to achieve desirable combinations of mechanical properties, with stiffness significantly higher than composites previously fabricated from similar materials using conventional methods. Nano-scale structures such as nano particles and nano layers have very high surface-to-volume ratios, making them ideal for use in composite materials and structures. Nanostructure ceramics are often both harder and less brittle than the same materials made on the scale of microns. Generally speaking, nano layer reinforcements distribute internal stresses more uniformly by allowing greater dimensional latitude in the forming and shaping processes, as compared to conventional macro-scale reinforcements.

Polyurea has been widely used as a coated material because of its extensive benefits and attractive properties. Polymers like polyurea are finding new applications in increasing the survivability of structures under impact loading, including those encountered in blast and ballistic events. Many researchers studied this behavior in the past. Polyurea offers a wide range in mechanical properties due to their ability to tailor the underlying hard and soft domain structure through chemistry. Due to the flexibility of these materials and their viability in a multitude of applications, their large deformation behavior over a wide range in strain rates is of

interest. As opposed to its rubbery behavior under low strain rates, polyurea displays a distinct leathery behavior at high strain rates (Sarva et al 2007). Previous experimental studies have revealed that the stress–strain behavior of polyurea depends on strain rate, temperature and pressure (Amirkhizi et al 2006 and Yi et al 2006). With the development of polyurea spray-coatings technology, specifically formulated polyurea can be directly and efficiently sprayed on the surface of structural components to enhance the mechanical strength and durability of civil and military structures (LI and Lua 2009). Improving ballistic performance of polyurethane foam by reinforcing it with nanoscale TiO<sub>2</sub> particles was reported in (Uddin et al 2009). Sandwich with nanophased cores absorbed about 20% more kinetic energy than their neat counterparts. The corresponding increase in ballistic limit was around 12% over the neat control samples. The penetration phenomenon was also monitored using a high-speed camera. Analyses of digital images showed that FSP remained inside the nanophased sandwich for about 7 microseconds longer than that of a neat sandwich demonstrating improved energy absorption capability of the nanoparticle reinforced core (Uddin et al 2009).

The main objective of this paper is to correlate micro/nano structure morphology to performance of Nano Particle Reinforced Polymers (NPRP) subjected to blast loading, to study the behavior of NPRP at high strain rates, and to evaluate the effect of the voids on the strain rate sensitivity of the materials.

## 2. NANO PARTICLE REINFORCED POLYMERS (NPRP)

Three polyurea-based elastomeric materials were investigated in this research: unreinforced polyurea; Exfoliated Graphene Nano Particle (xGnP) reinforced polyurea; and Polyhedral Oligomeric Silsesquioxane (POSS) reinforced polyurea. The polyurea used in this study was LINE-X XS- 350 produced by Protective Coatings Inc., POSS was provided by Hybrid Plastic

Inc. and xGnP was manufactured by XG-Sciences.

### *2.1. Exfoliated Graphene Nano Particle (xGnP)*

Since the late 1990's, research has been reported that intercalated, expanded, and/or exfoliated graphite nanoplatelets could also be used as nano-reinforcements in polymer systems. The key point of utilizing graphite as a nano-reinforcement is in its ability to exfoliate using Graphite Intercalated Compounds (GICs). Natural graphite is abundant and its cost is low compared to the other nanosized carbon materials. The graphite nanoplatelets are expected to be marketed at approximately \$10-20/lb once high demand and full production is achieved. This is significantly less expensive than single wall nanotubes (SWNT) (>\$45,000/lb) or vapor grown carbon fiber (VGCF) (\$40-50/lb), yet the mechanical, electrical, and thermal properties of crystalline graphite flakes are comparable to those of SWNT and VGCF.

These nanoplatelets are typically less than 5 nm thick and can be synthesized with lateral dimensions ranging from less than 1  $\mu\text{m}$  to up to 100  $\mu\text{m}$ . The graphite nanoplatelets have large intrinsic fracture energy since their modulus is over 1 TPa, and they can undergo a large out-of-plane deformation before fracture. Thus, these graphite nanoplatelets could be an alternative, cost-effective material for carbon nanotubes. The use of exfoliated graphite flakes (xGnP) opens up many new applications where electromagnetic shielding, electrical conductivity, high thermal conductivity, gas barrier resistance, high fracture toughness, or low flammability is required.

The addition of xGnP to a polymer cannot be expected to provide much of an enhancement of the fracture properties of the polymer matrix unless the adhesion of xGnP to the matrix is optimized, the concentration is high, and the size is large. In that way, xGnP can add its high intrinsic fracture energy to assist the polymer fracture resistance if xGnP can bridge across the

growing crack front. Patented exfoliated graphite nanoplatelets (xGnP) were produced at Michigan State University. XGnP-15, made from Asbury 3772 using High Power Microwave was used. Prior to its use, xGnP platelets were kitchen-microwaved for 1 min/1min per 10-15 g.

## 2.2. Polyhedral Oligomeric Silsesquioxane (POSS)

Polyhedral Oligomeric Silsesquioxane (POSS<sup>®</sup>) is a class of silicon based nanochemicals designed to fulfill various mechanical functions. POSS<sup>®</sup> nanochemicals represent a sophisticated example of true molecular level assembly and are being hailed as the revolutionary next big leap in nanomaterials' technology. They are the first entirely new chemical feedstock to have been developed in the last 50 years. They are affordable, cost competitive, and represent a recyclable polymer feedstock. It marries the beneficial properties of three materials: plastics (processability and toughness), ceramics (thermal, chemical and oxidative stability) and metals (radiation absorption, catalysis, refractive index, and conductivity).

The hybrid (organic/inorganic) composition of POSS technology enables it to occupy a very unique and dramatically enhanced property space relative to material building blocks. An important benefit is that it imparts material formulations containing POSS with excellent thermal, oxidative, and environmental stability and toughness. This is largely due to the inorganic component. The organic portion of their composition provides compatibility with polymers, thereby, enabling their facile incorporation into all polymeric resin systems.

In addition to improving the performance of polymers, POSS has also seen extensive systematic development. Full control over the cage size, compatibility, purity and functionality has been achieved. POSS is currently the only nanomaterial technology qualified for use in electronic components with a 99.9% control over purity and quality demonstrated on a commercial basis of tons per year production.

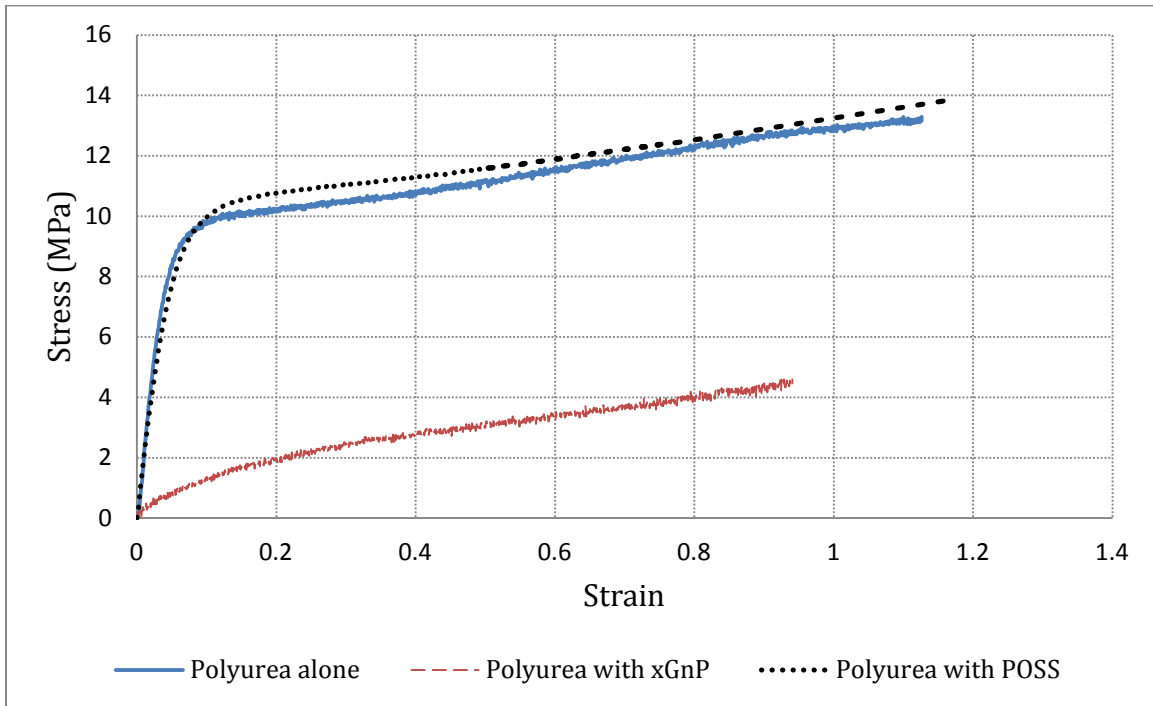
POSS dispersion is thermodynamically governed by the free energy of mixing equation ( $\Delta G = \Delta H - T\Delta S$ ). The nature of the R group and ability of the reactive groups on the POSS/POMS cage to react or interact with polymers and surfaces greatly contributes to a favorable enthalpic ( $\Delta H$ ) term, while the entropic term ( $\Delta S$ ) for POSS/POMS is also highly favorable because of the monoscopic cage size and distribution of 1.0. The thermodynamic forces driving dispersion are also contributed to by kinetic mixing forces, such as those occurring during high shear mixing, solvent blending or alloying. POSS/POMS building blocks provide the potential to incorporate metals into polymers without the limitations of viscosity increases, loading levels, agglomeration, and opacity that plague traditional filler technologies. *POSS<sup>®</sup> Molecular Silicas<sup>™</sup> show the revolutionary capacity to be tailored to nearly any conventional polymer system*, and, additionally, demonstrate the amazing ability to be loaded at 50wt% levels while maintaining optical transparency and processability (Lichtenhan et al 2001).

### 2.3. Experimental Program

The tensile stress-strain response for these materials under quasi-static conditions was determined in (Irshidat et al). Modulus of elasticity, tensile strength, and strain at failure were also obtained from the stress-strain curves for each material. Typical stress-strain curves and typical mechanical properties of these materials are shown in Figure 1 and Table 1 respectively.

**Table 1** Retrofitted materials properties (Irshidat et al)

Material	Modulus of Elasticity (MPa/ psi)	Ultimate Strength (MPa/ psi)	Strain at Rupture (%)	Strain Energy (MPa)
Polyurea	229/ 33280	13.3/1927	113	12.5
Polyurea with xGnP	12.1/1749	4.6/666	94	2.7
Polyurea with POSS	210/30539	13.8/2003	116	13.3



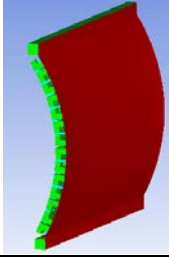
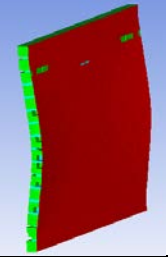


**Fig. 1** Typical stress-strain relation for NPRP materials under tensile loading (Irshidat et al)

Irshidat et al. 2010 concluded that adding POSS particles to reinforce polyurea affected neither the strength nor the stiffness of the unreinforced polyurea under quasi-static conditions. However, adding xGnP particles clearly decreased both the strength and the stiffness of the unreinforced polyurea. Both the neat polyurea and polyurea reinforced with POSS had very similar stress-strain curves under quasi- static conditions (Figure 1) with slightly higher strain energy for the POSS reinforced polyurea compare to neat polyurea (Table 1). On the other hand, xGnP reinforced polyurea absorbed less strain energy than the other two materials.

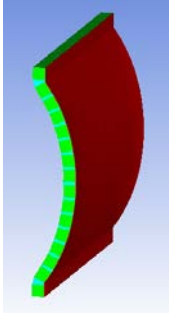
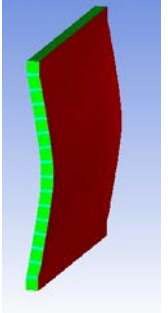


Three CMU walls were tested at the US Army Engineer Research and Development Center (ERDC) using a blast simulator (Irshidat et al). The sample walls were retrofitted with: (1) unreinforced polyurea (2) reinforced polyurea with xGnP, or (3) reinforced polyurea with POSS, respectively. A spraying technique was used to apply polyurea or nano-reinforced polyurea to the

back (interior face) of the CMU walls. A pre-adjusted air blast pressure and impulse were applied to each wall. Test results showed that the wall retrofitted with polyurea alone failed (Table 2) while the wall retrofitted with POSS reinforced polyurea and subjected to same loading condition (e.g. blast) did not fail (Table 3). Therefore both materials had different behaviors and different properties under different strain rate conditions (strain-rate dependent). This conclusion magnifies the need for carrying out a more comprehensive evaluation of this issue. A crucial question arises: “will the morphology of these materials at nano scale play a role on their performance under different loading conditions?”

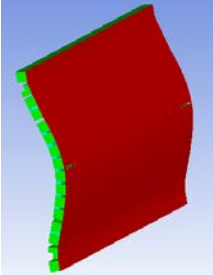
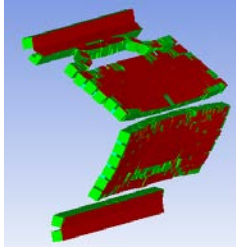


**Table 2** Numerical and experimental results comparison for the case of CMU wall retrofitted with polyurea (Irshidat et al)

Beginning of the Failure	Final Stage	
		<p>Numerical Results obtained using AUTODYN hydrodynamic code</p>
		<p>Experimental results obtained using BLS</p>

**Table 3** Numerical and experimental results comparison for the case of CMU wall retrofitted with POSS reinforced polyurea (Irshidat et al)

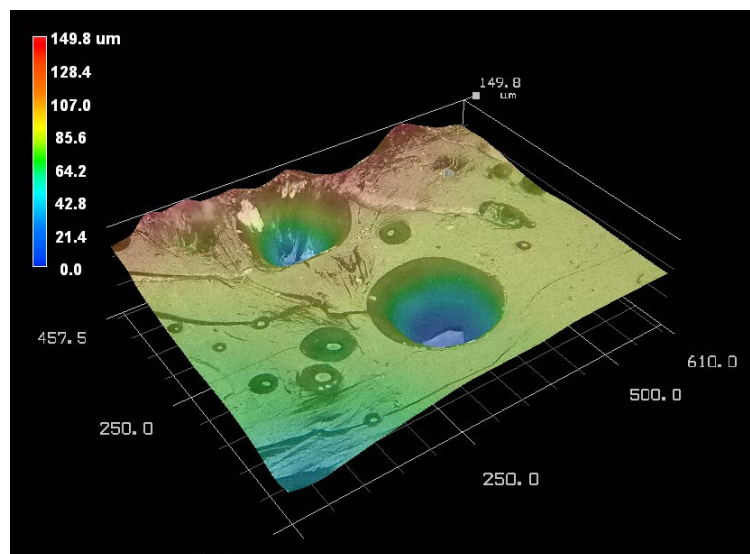
Maximum deflection	final stage	
		Numerical Results obtained using AUTODYN hydrodynamic code
		Experimental results obtained using BLS

**Table 4** Numerical and experimental results comparison for the case of CMU wall retrofitted with xGnP reinforced polyurea (Irshidat et al)

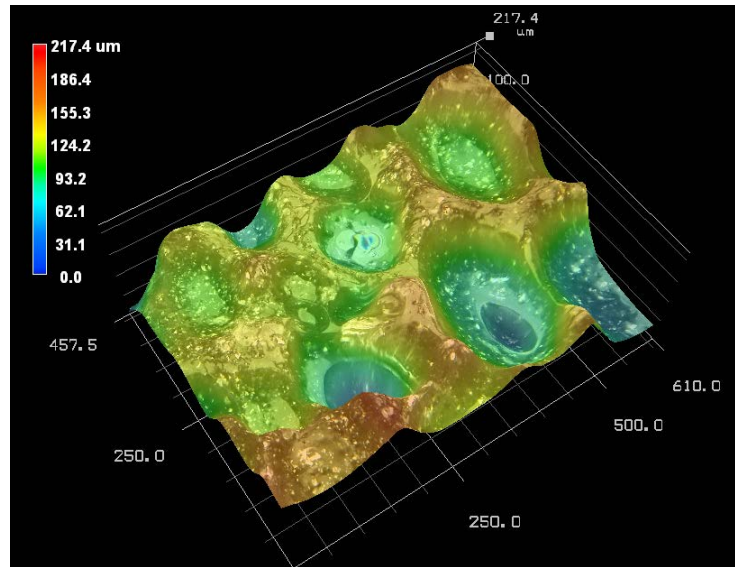
Beginning of the Failure	Final Stage	
		Numerical Results obtained using AUTODYN hydrodynamic code
		Experimental results obtained using BLS

Fractal analysis is a well-known method which is widely used. The main concept of fractal analysis is that a fractal dimension can be considered as a quantitative measure of object surface

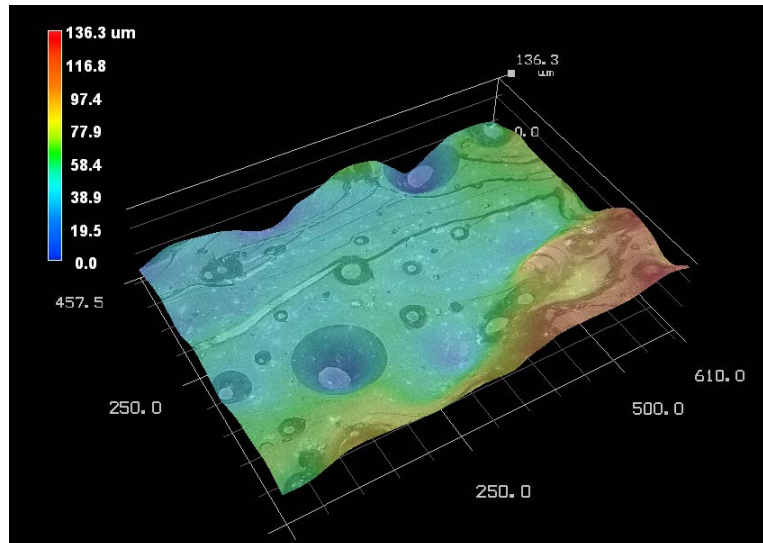
heterogeneity because of its inherent self-similarity features. In other words, one could interpret the fractal dimension as a measure of heterogeneity of a set of points on a plane, or in space. In case of fractured surfaces, the fractal dimension is viewed as a measure of surface roughness. In this study, 3D- microscopic imaging was conducted on polyurea, xGnP polyurea, and POSS reinforced polyurea using KEYENCE Digital Microscope, Model: VHX-600 with 500 x magnification at 10 um contour steps (Figure 2 and Table 5). The results show that the normalized fracture surface area, which equal the total fractured surface divided by projected gross area, for POSS reinforced polyurea was greater than it for plain polyurea as expected. On the other hand, the fractured surface area for xGnP reinforced polyurea was found to be much larger than the other two materials. Further evaluation of the fractured images (Figure 2) shows that the xGnP reinforced polyurea has the largest amount of voids. Subtracting the surface area of voids and considering only the net fractured surface area will result in much smaller area for the xGnP reinforced polyurea. This preliminary investigation magnifies the need for carrying out a more comprehensive evaluation of voids effect which is discussed in details next section.



(a)



(b)



(c)

**Fig.2** Scanning electron micrograph of fracture surface of (a) polyurea, (b) xGnP reinforced polyurea, and (c) POSS reinforced polyurea

**Table 5** scanning electron microscopic results

	Scanned area (um <sup>2</sup> )	Fracture surface area (um <sup>2</sup> )		Normalized fracture surface area	
		Gross	Net	Gross	Net
Polyurea	279441	306748	217165	1.10	0.78
xGnP reinforced polyurea	279441	416119	158073	1.50	0.57
POSS reinforced polyurea	279441	319073	247065	1.14	0.88

### 3. 3-D-CT SCAN IMAGING

Polyurea-based elastomeric materials were examined as potential retrofit materials. Polyurea matrix was selected because of its low viscosity and the high degree of property control by way of the selection of curing agents and processing temperatures. The selected nano-reinforced polyurea was applied to Concrete Masonry Units (CMU) using the spraying technique mentioned in (Irshidat et al). The result obtained from CMU blast testing showed premature and unexpected levels of failure that did not match theoretical expectations (Tables 2-4).

In order to gain insight into failure mechanisms, tomography was conducted on polyurea, xGnP reinforced polyurea, and POSS reinforced polyurea using 3D CT scan, SkyScan 1172 scanner, at 2-micron resolution. The samples were lined up abreast on the 2 cm wide Skyscan stage and scanned using the camera offset setting with a 3,961 micron vertical height. The scan was set up using the oversize and multiple scans tool. Although not necessary, this will enable more clear identification of the portion of the object being scanned. Before beginning the scan, a new flat-field correction was taken with X-ray tube settings of 40 kilovolts and 250 micro amps using a 1,767 millisecond camera exposure. One hundred (100) slice representative datasets, consisting of lines 180 (0.367 mm) to 280 (0.572 mm), were used for 3-D pore size analyses. 3-D models were made from these same data sets. The results of the 3D CT imaging showed a large number of voids as shown in Figure 3. Void size, shape and distribution (Figure 4) were found to be random within scanned materials which magnified the need for carrying out a more comprehensive statistical evaluation of defect (e.g. voids) distribution.

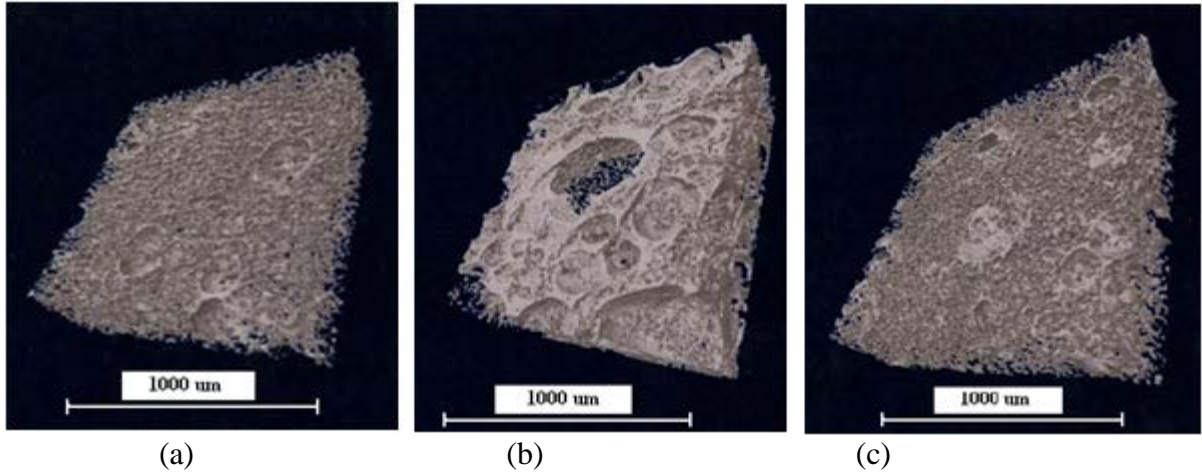


**Fig. 3** Typical obtained 3D micro CT scan using Sky Scan 1172 model showing micro sized voids of (a) polyurea, (b) polyurea reinforced with xGnP, and (c) polyurea reinforced with POSS



**Fig. 4** Voids in xGnP reinforced polyurea

#### 4. STATISTICAL EVALUATION OF VOID DISTRIBUTION

The 3D-CT scan imaging results showed that the three tested NPRP had voids with various sizes and different probability distributions as shown in Figure 5.

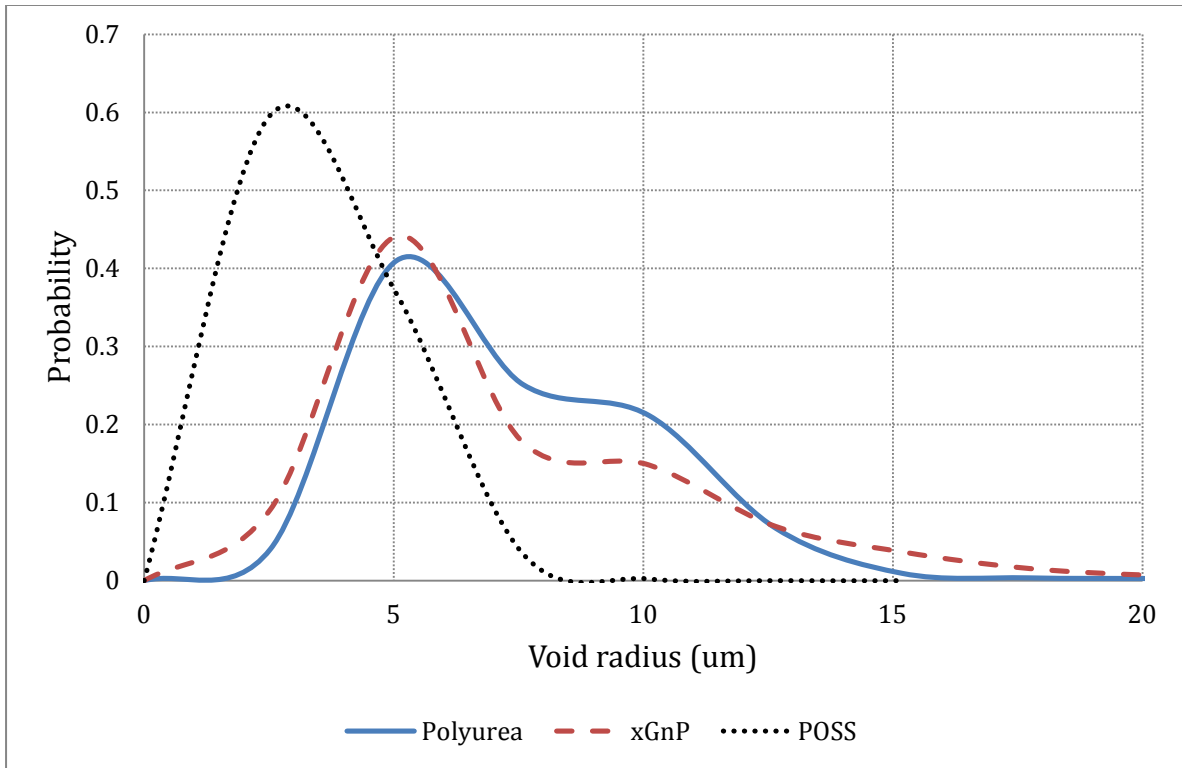


**Fig. 5** Probability distribution of voids inside NPRP

**Table 6** Statistical evaluation of the void distribution inside the materials

	Plain polyurea	xGnP reinforced polyurea	POSS reinforced polyurea
Void mean	7.34	7.53	3.65
Void standard deviation	3.01	4.29	4.05
Void maximum radius (micro meter)	30.37	48.08	15.18
Void Minimum radius (micro meter)	2.53	2.53	2.53

Polyurea specimen has 31211 voids distributed randomly. The radius of these voids ranges between 2.53 and 30.37 micro meters with a mean of 7.43 micro meters and standard deviation of 3.01 (Table 6). xGnP reinforced polyurea specimen has 18783 voids distributed randomly.

The radius of these voids ranges between 2.53 and 48.08 micro meters with a mean of 7.53 micro meters and standard deviation of 4.29. POSS reinforced polyurea specimen has 45166 voids distributed randomly. The radius of these voids ranges between 2.53 and 15.18 micro meters with a mean of 3.65 micro meters and standard deviation of 4.05.

It was clear that the POSS reinforced polyurea has the largest number but the smallest sized voids among the three tested materials: whereas, the xGnP reinforced polyurea has the lowest number but the largest sized voids. It was also clear that polyurea and xGnP reinforced polyurea have voids randomly distributed within a wide range, while POSS reinforced polyurea has voids randomly distributed within a narrow range. It is important to note that about 60% of the void distributed inside the POSS reinforced polyurea specimen have radii of 2.53 micro meters (the smallest void size): whereas about 41% and 44% of the void distributed inside the polyurea and xGnP reinforced polyurea specimens, respectively, have radii of 5.06 micro meters. The statistical evaluation results show that the void's size and distribution may have an important role in the behavior of NPRP under different loading conditions. The next section covers in detail the effect of the voids on the performance of these materials.

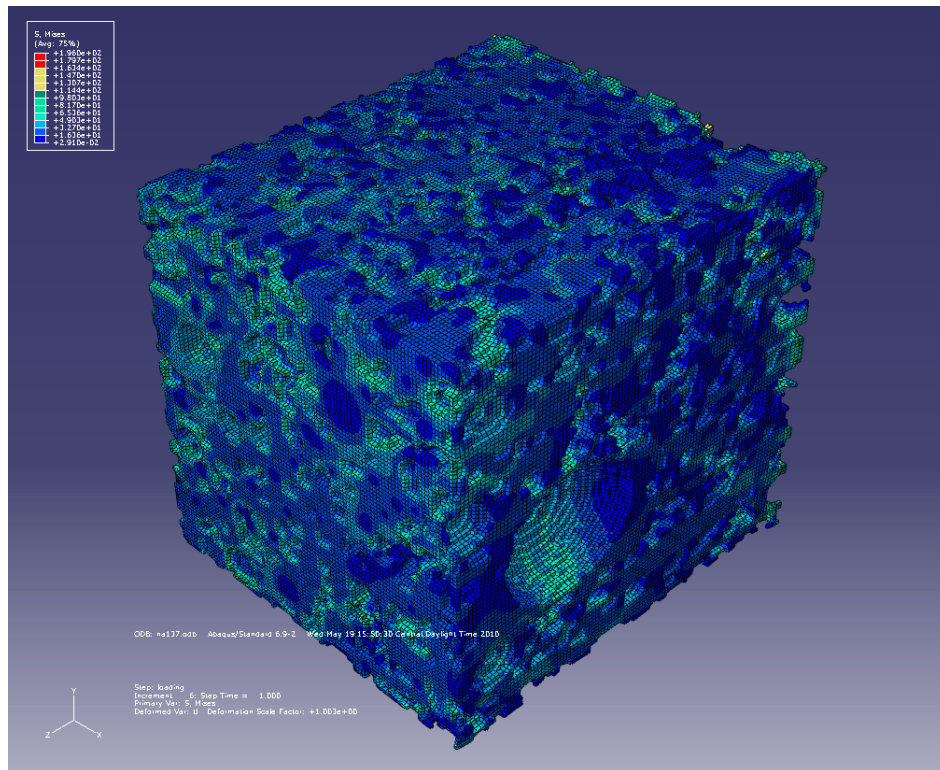
## 5. VOIDS EFFECT ON NPRP BEHAVIOR-COMPUTATIONAL ANALYSIS

In this section, three dimensional finite element (FE) simulations were performed in order to develop an understanding for the voids effect and the strain rate sensitivity of nano particle reinforced polymers. Two methods were used in this research: real volume element and representative volume element.

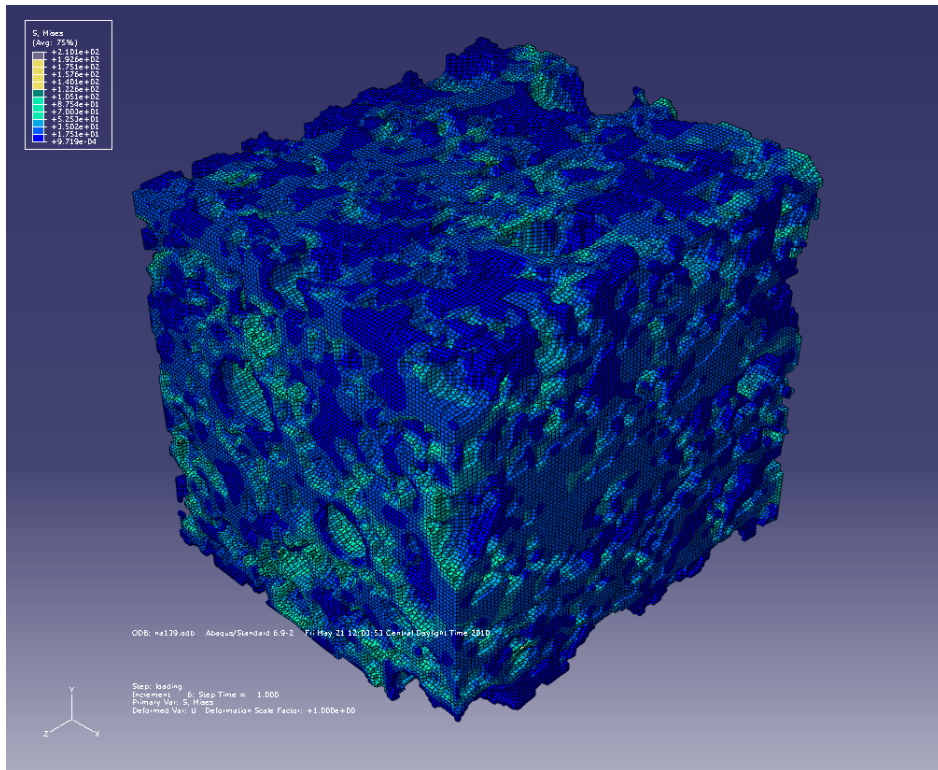
### 5.1. *Real Volume Element*

Detailed 3D-CT scan images obtained using SkyScan instrument were mapped to finite element code using Mimic Software. In this part of the study, commercially available ABAQUS

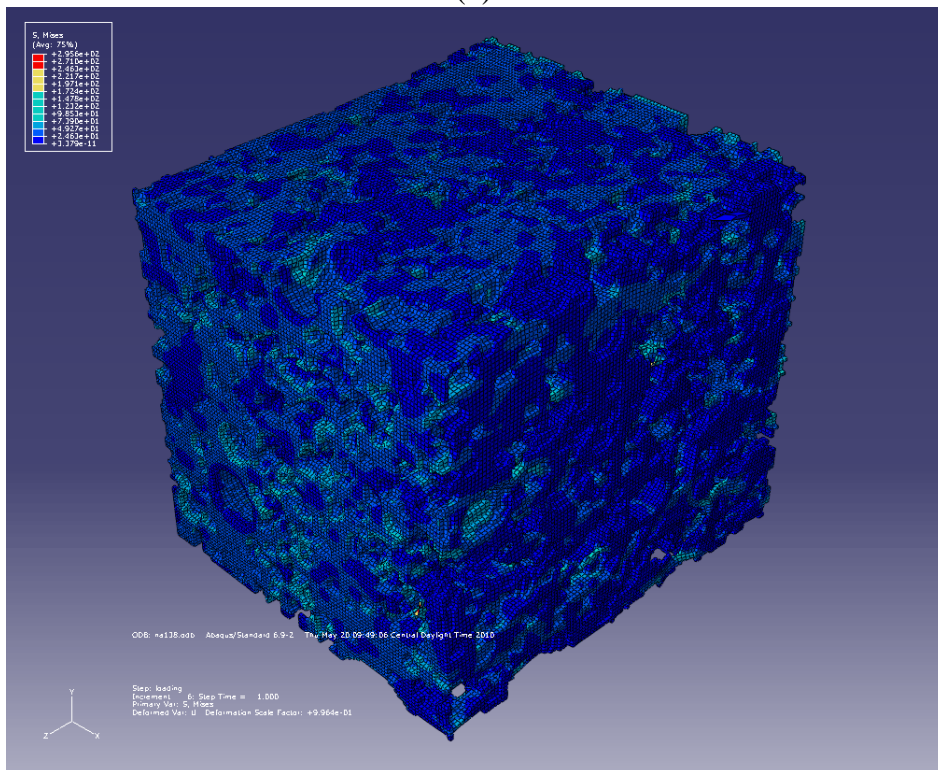
software version 6.9-2 was employed. 8-node brick element was used in the analysis. 812592, 659324, and 728117 elements were used to build the finite element mesh for polyurea, xGnP reinforced polyurea, and POSS reinforced polyurea respectively. Displacement boundary condition was applied in the vertical direction. The results (Figure 6) show that the stress was not uniform, but rather localized and not evenly distributed around voids.



(a)



(b)



(c)

**Fig. 6** Von-Mises stress distribution due to static loading (a) Polyurea alone (b) xGnP reinforced polyurea (c) POSS reinforced polyurea

A statistical evaluation was carried out to study the stress distribution inside the specimens. The results are summarized in Figure 7 and Table 7. Figure 7 shows that the Von-Mises stress was randomly distributed through the elements for all specimens with means equal to 27.15, 23.12, and 25.66 and standard deviations equal to 8.29, 9.77, and 9.27 for polyurea alone, xGnP reinforced polyurea, and POSS reinforced polyurea, respectively (Table 7).

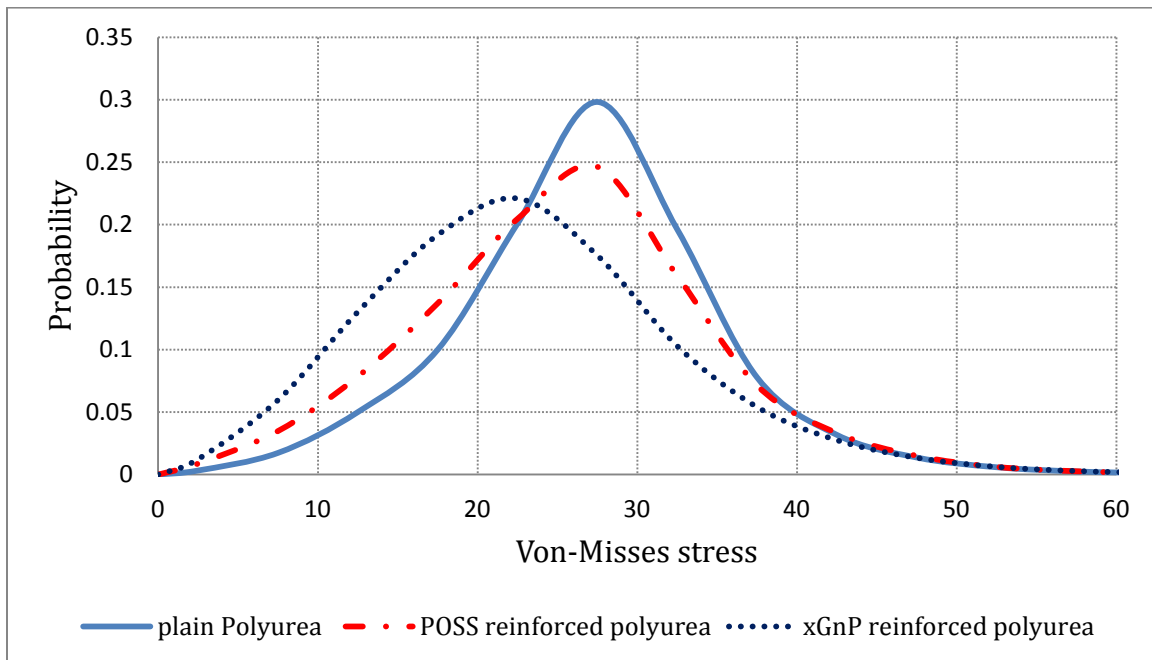


**Fig. 7** Probability distributions of Von-Mises stress in the elements

**Table 7** Statistical evaluation of stress distribution inside the elements

	Plain polyurea	xGnP reinforced polyurea	POSS reinforced polyurea
Mean	27.2	23.1	25.7
Standard deviation	8.3	9.8	9.3
Maximum stress	130	141	235
Minimum stress	0.01	0	0

## 5.2. Representative Volume Element

Complete detailed modeling of polyurea-based elastomeric materials is usually a complicated, tedious, and time consuming effort. Parametric evaluation of the effect of void ratio and void size was conducted. In the parametric evaluation, polyurea material was modeled by using a representative volume element (RVE) to simplify computational limitations.

The 3-D-CT scan imaging results showed that the void's size and ratio may play a major role in the behavior of the NPRP. In order to study the effect of these two factors, dynamic nonlinear explicit finite element code AUTODYN was used to perform three- dimensional analyses for the representative volume element model.

### 5.2.1. Void's Size Effect

To study the effect of void's size on the NPRP stress-strain behavior under high strain rates, 30  $\mu\text{m}$  representative volume element models were created. In order to obtain the actual void ratio of the materials, which is 0.28, the research team randomly generated spherical voids of 42, 12, and 4 with radii of 3.5, 5, and 7.5  $\mu\text{m}$ , respectively (Figure 8). A strain rate of  $50000\text{s}^{-1}$  was applied in the vertical direction of the model.

The results show that the stress decreases with an increasing radius of the voids inside the specimen when it is subjected to high strain rates (Figure 9). This reduction in the stress was about 13%, 24%, and 34% when the radius of the void increase from 3.5 to 5, 5 to 7.5 and 3.5 to 7.5 micrometer respectively (Table8). For a given applied strain/ displacement, it is clear that when the size of the void increases, the average resulting stress decreases which results in reduction in stored energy (Figure 9). These results support the blast experimental findings wherein the wall coated with polyurea alone failed under blast, while the wall coated with POSS reinforced polyurea did not. The 3-D CT scan imaging showed that the POSS reinforced

polyurea has voids with  $3.5 \mu\text{m}$  radius in average, while polyurea alone has voids with  $7.5 \mu\text{m}$  radius on average.

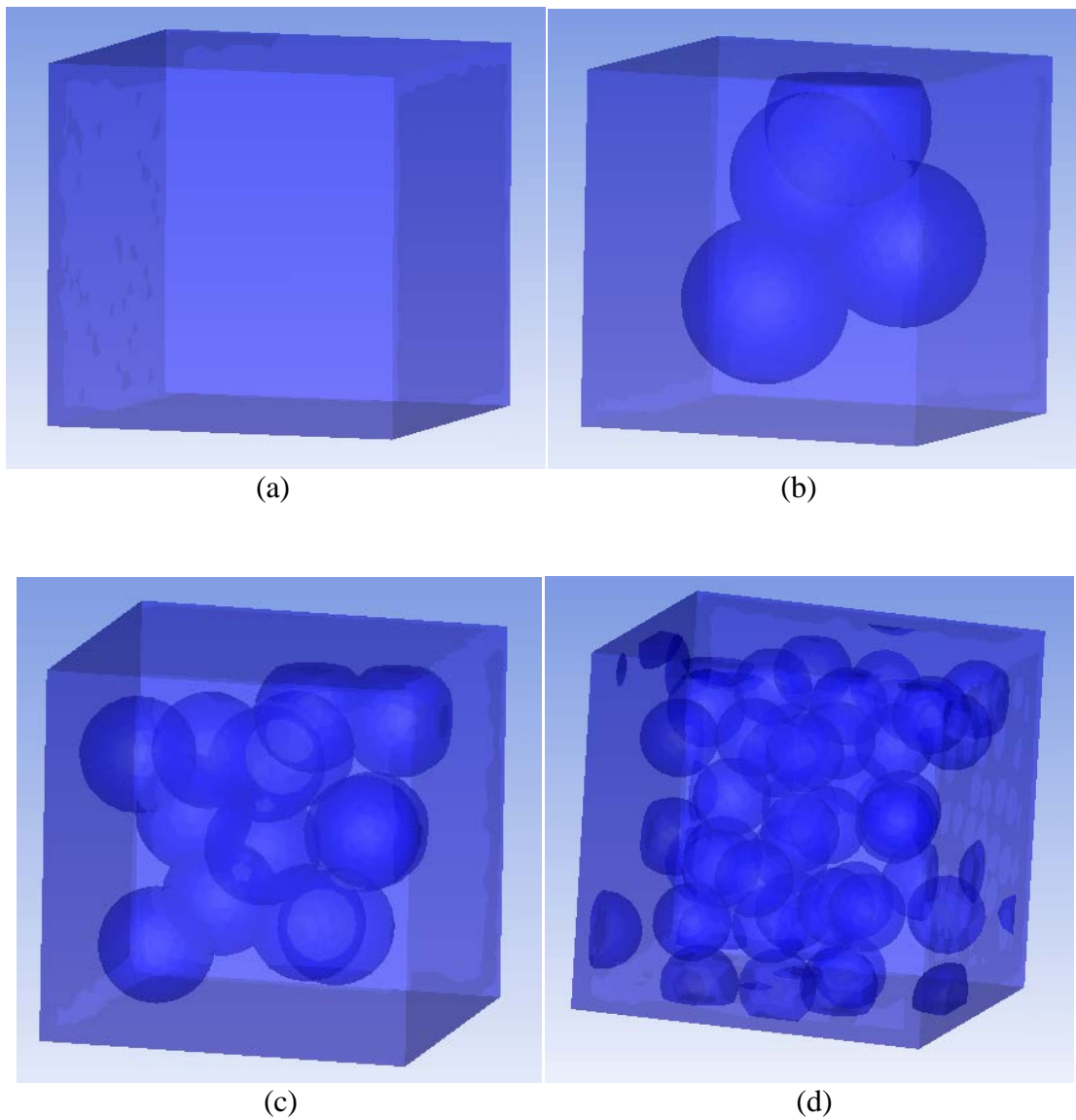


**Fig. 8** Spherical voids generated (a) no void (b) 4 voids of  $7.5\mu\text{m}$  radius (c) 14 voids of  $5.0\mu\text{m}$  radius (d) 42 voids of  $3.5\mu\text{m}$  radius

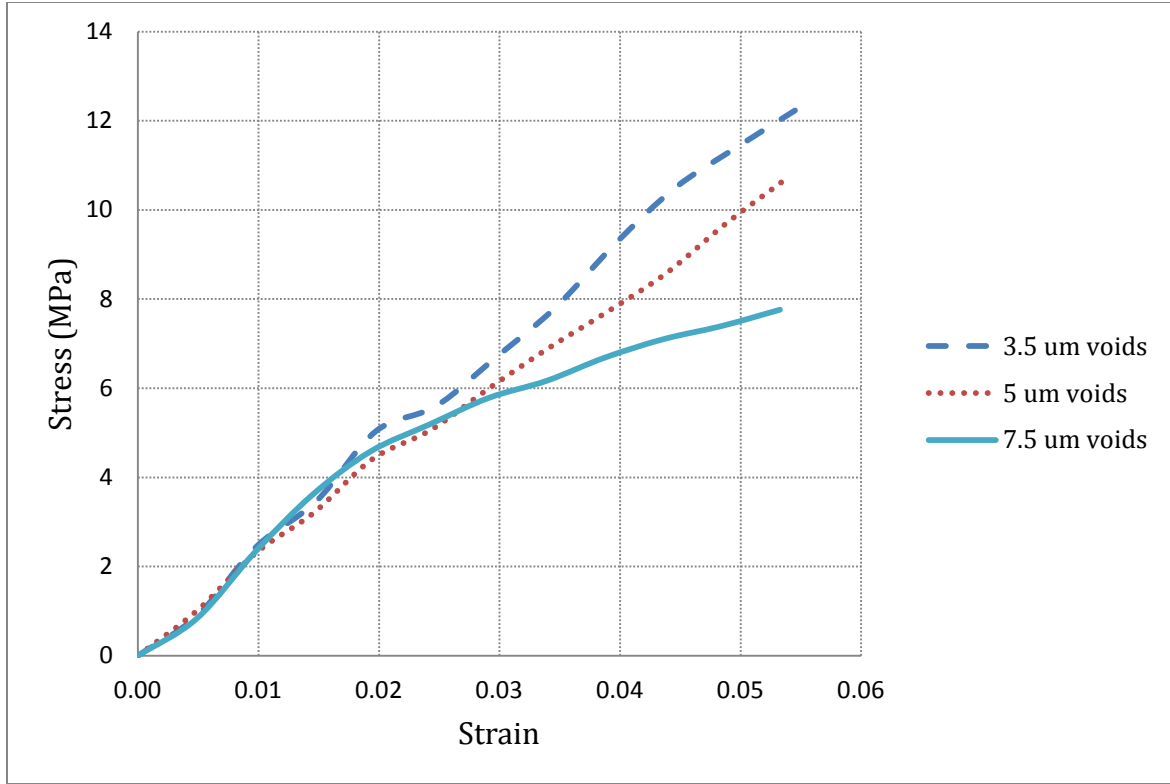


**Fig. 9** Stress-strain curve for specimens with 0.28 void ratio and different void radius subjected to  $50000\text{s}^{-1}$

**Table 8** Stress value at 0.05 strain for specimens with 0.28 void ratio and different void radius subjected to  $50000\text{s}^{-1}$

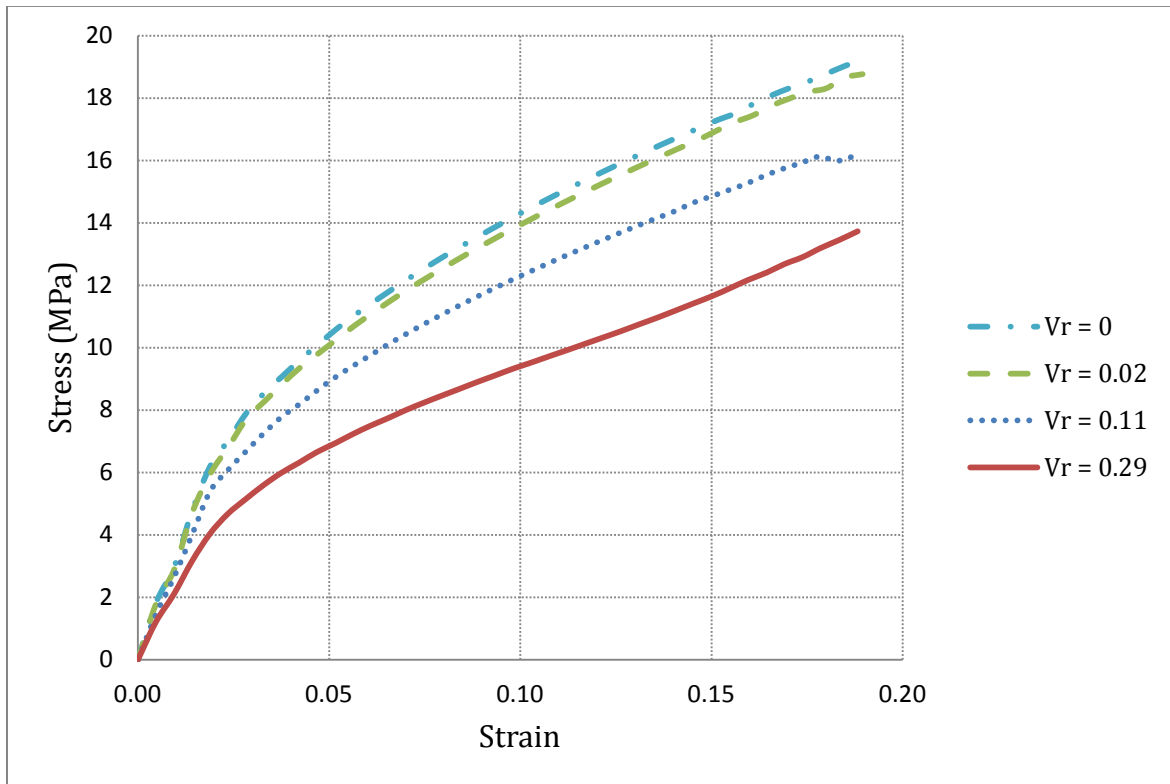
Void radius (um)	Stress at 0.05 strain (MPa)	Percent reduction (%)	
3.5	11.46	13.28	34.44
5	9.94		
7.5	7.51	24.39	

### 5.2.2. Void Ratio Effect on Strain Rate Sensitivity of NPRP

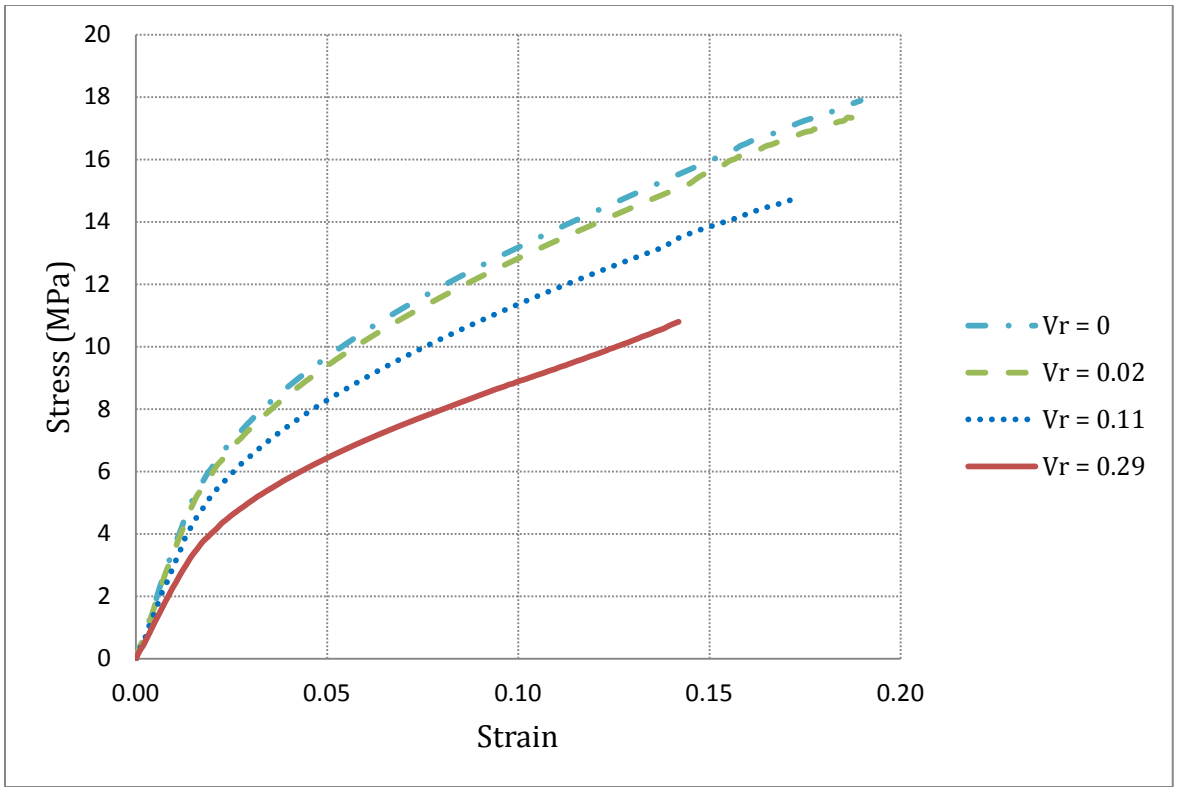
In order to study the effect of void ratio on the strain rate sensitivity of NPRP, a series of simulations was conducted for 20 um representative volume element models with different numbers of 3.5 um voids randomly generated inside the specimen. 0, 0.02, 0.11, and 0.28 void ratios were taken into consideration. The void radius was kept constant, 3.5 um, for all

simulations to negate the void size effect. Strain rates of  $50000\text{ s}^{-1}$ ,  $10000\text{ s}^{-1}$ , and  $1000\text{ s}^{-1}$  were applied in the vertical direction to investigate the strain rate sensitivity of the NPRP.

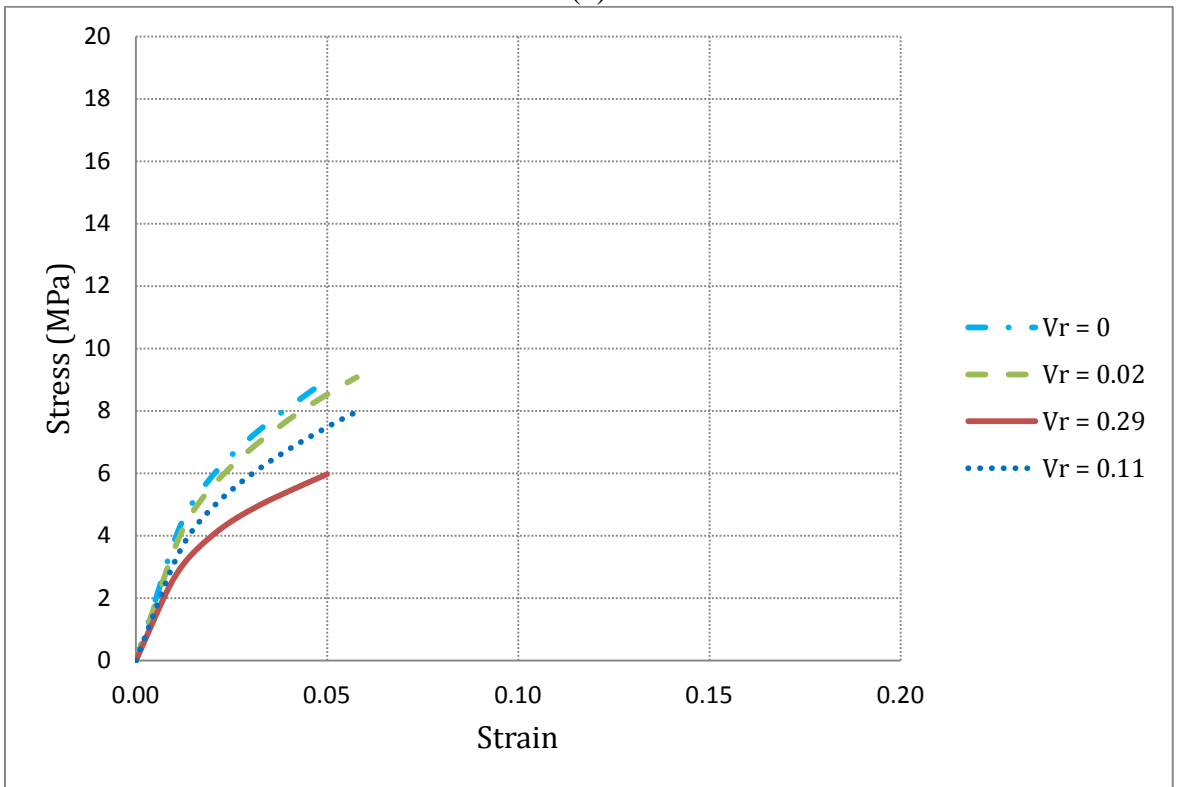
The results show that the average stress decreases with increasing void ratio inside the specimen for all applied strain rates (Figure 10). The mechanical behavior depends on strain rate as illustrated in Figure 11. Figure 12 presents the rate-dependence of the stress–strain behavior in a form of stress vs. logarithm strain rate, taking the stresses evaluated at strain level of 0.05. It clearly demonstrates a close-to-linear dependence on the logarithm of the strain rate. However, the linear relationship at various void ratios reveals that the rate dependence mechanism depends on the void ratio.



(a)

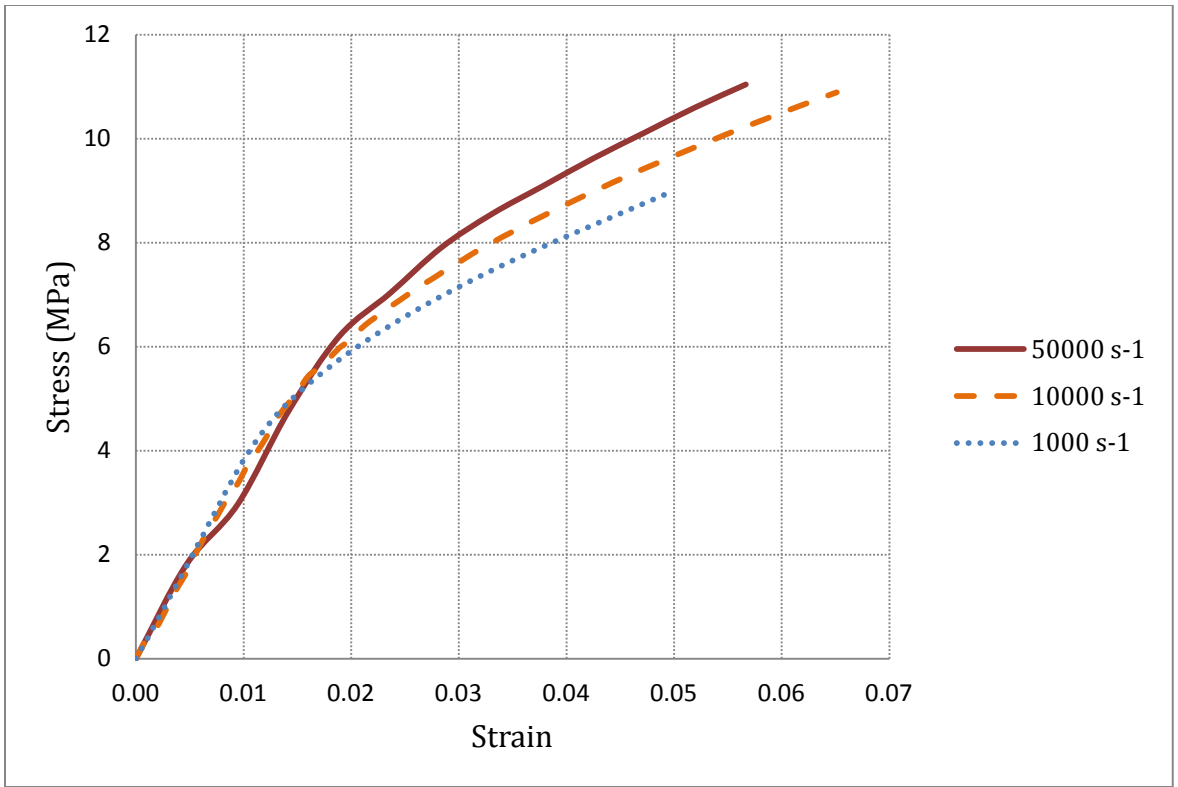


(b)

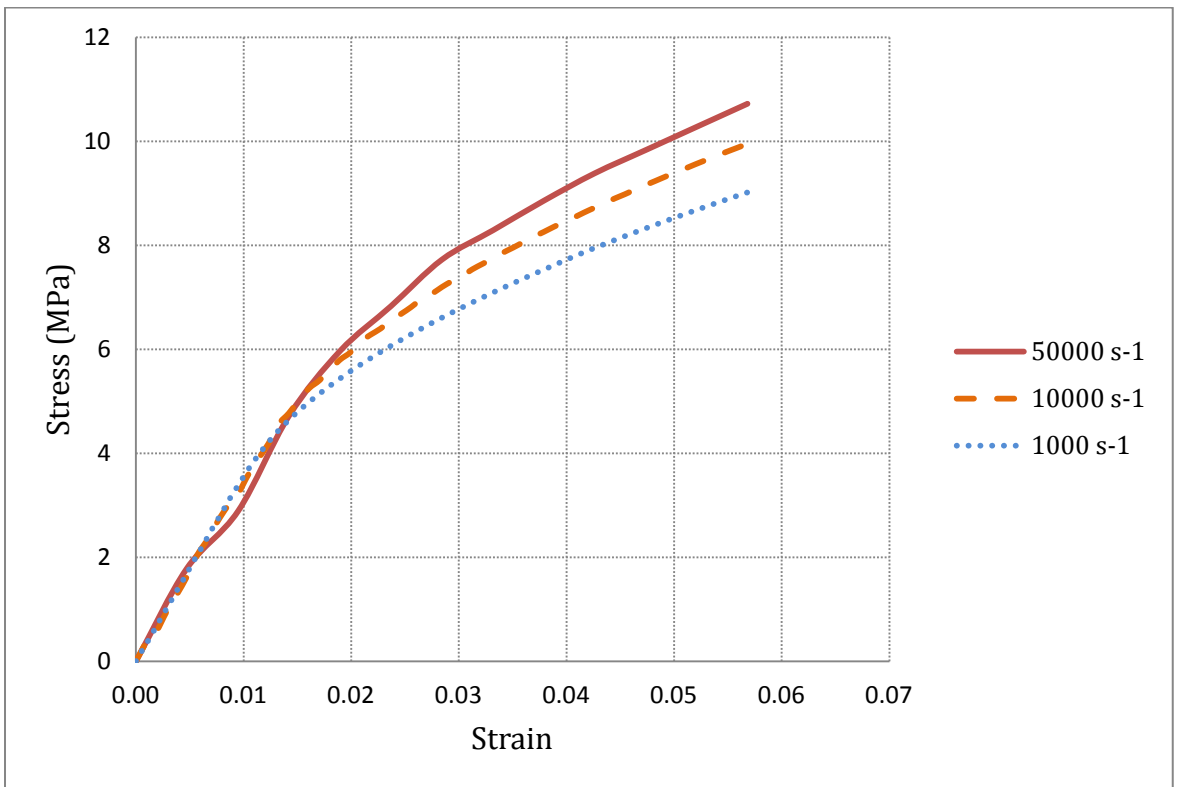


(c)

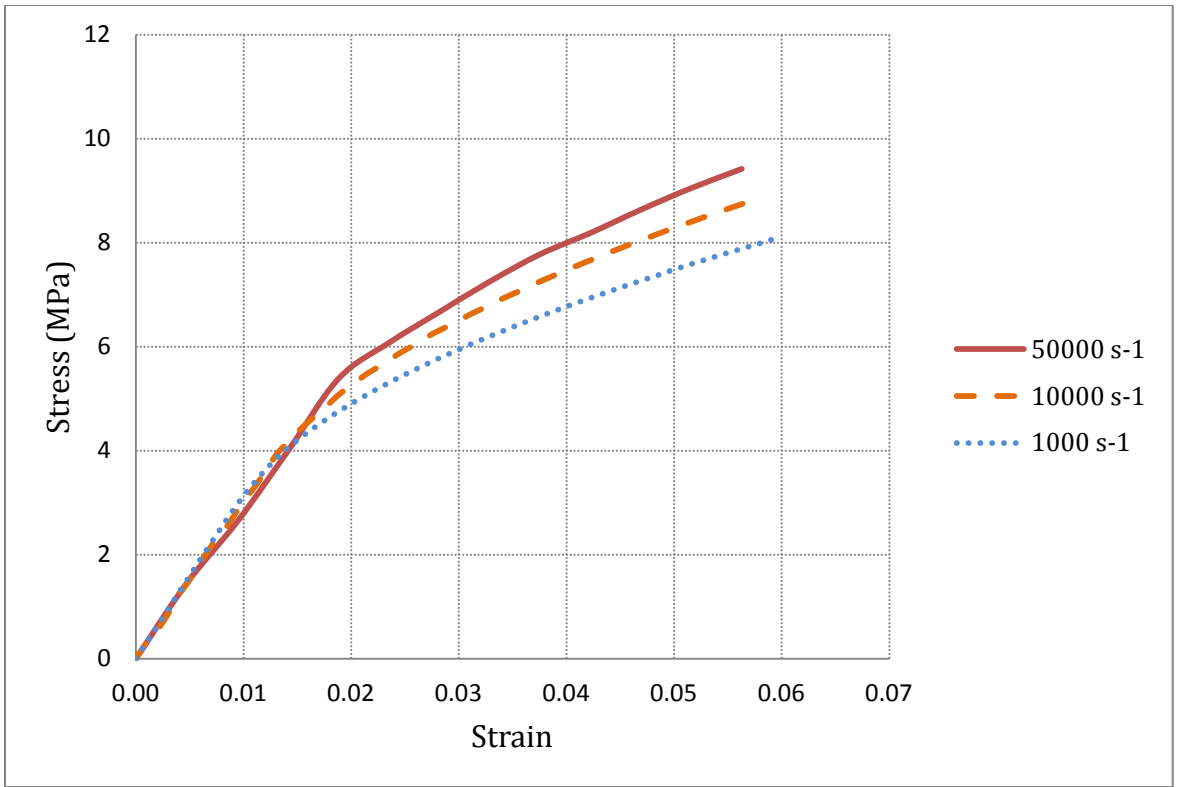
**Fig. 10** Void ratio effect on stress-strain behavior of NPRP subjected to (a) 50000s<sup>-1</sup> (b) 10000s<sup>-1</sup> (c) 1000s<sup>-1</sup>



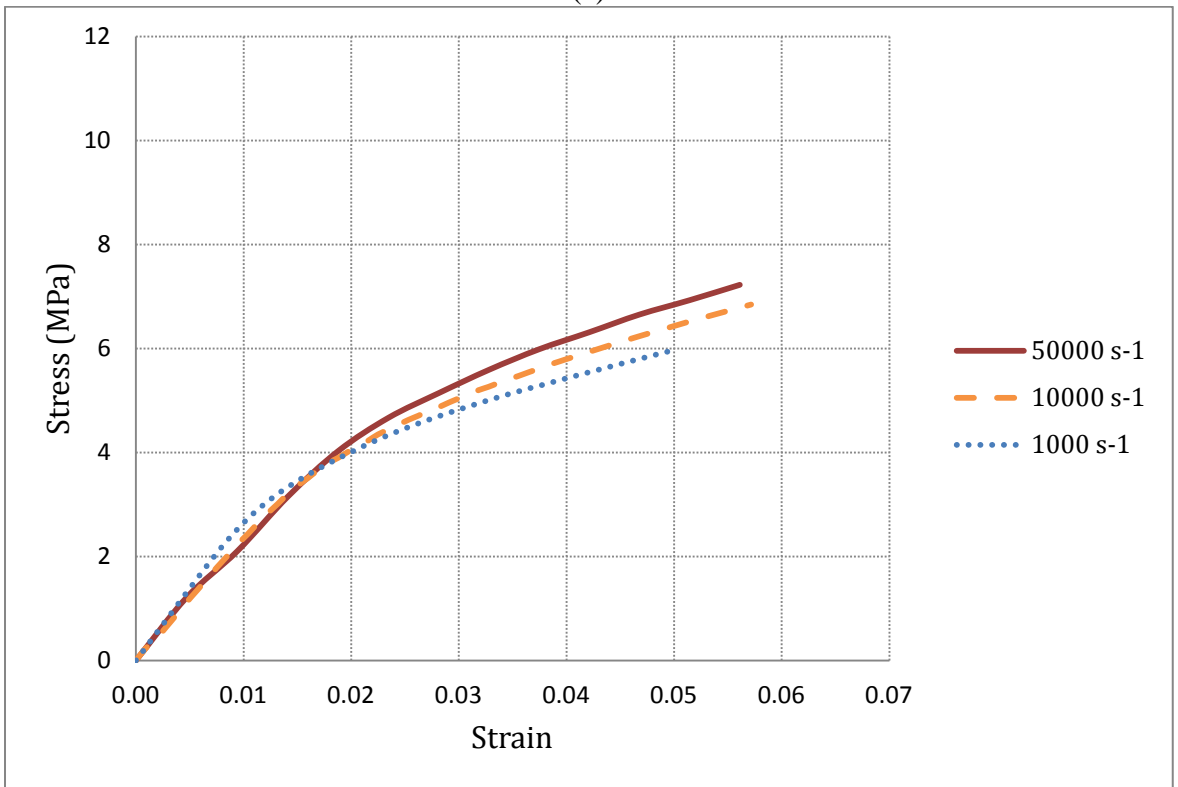
(a)



(b)



(c)



(d)

**Fig. 11** Strain rate effect on stress-strain behavior of NPRP with void ratio of (a) 0 (b) 0.02 (c) 0.11 (d) 0.28

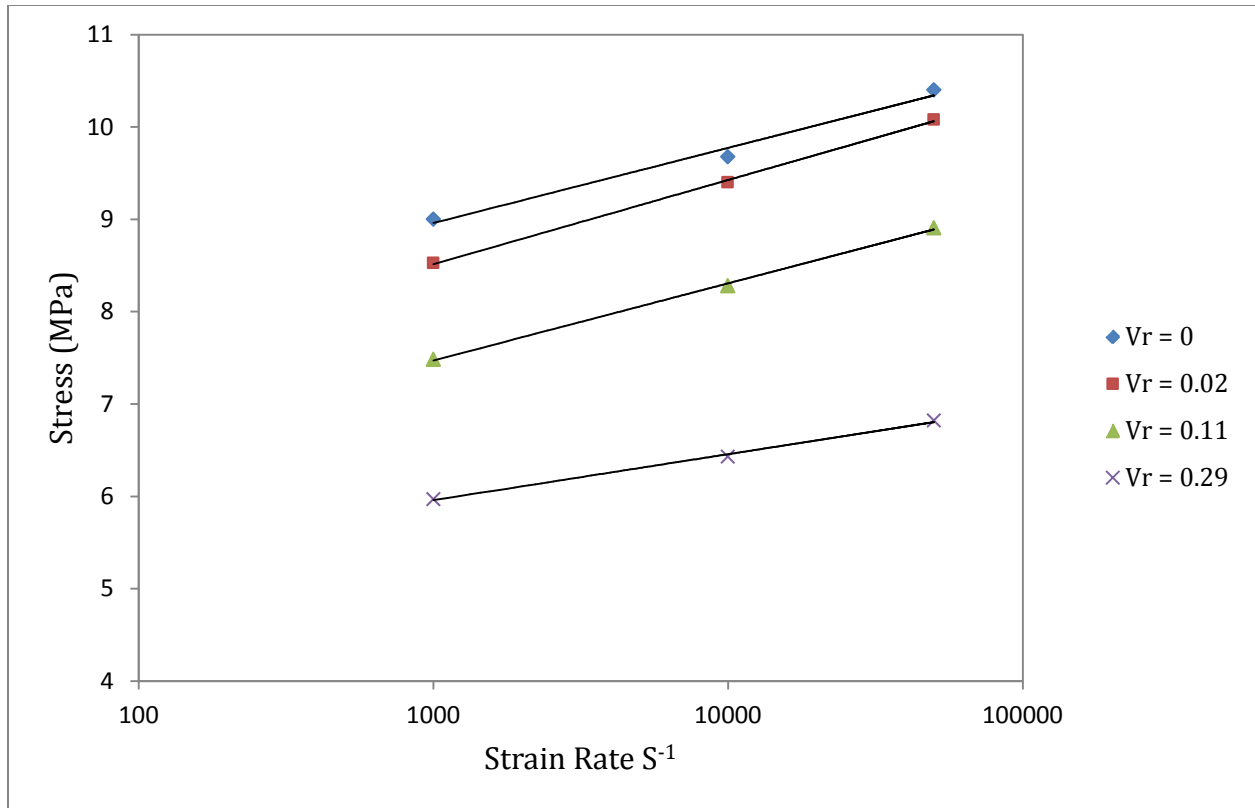


**Fig. 12** Stress vs. strain rate of NPRP with different void ratio at strain 0.05

Figure 13 shows the void ratio-dependence of the stress–strain behavior in a form of stress vs. void ratio, taking the stresses evaluated at strain level of 0.05. It clearly demonstrated a close-to-exponential dependence of the void ratio for all applied strain rates.

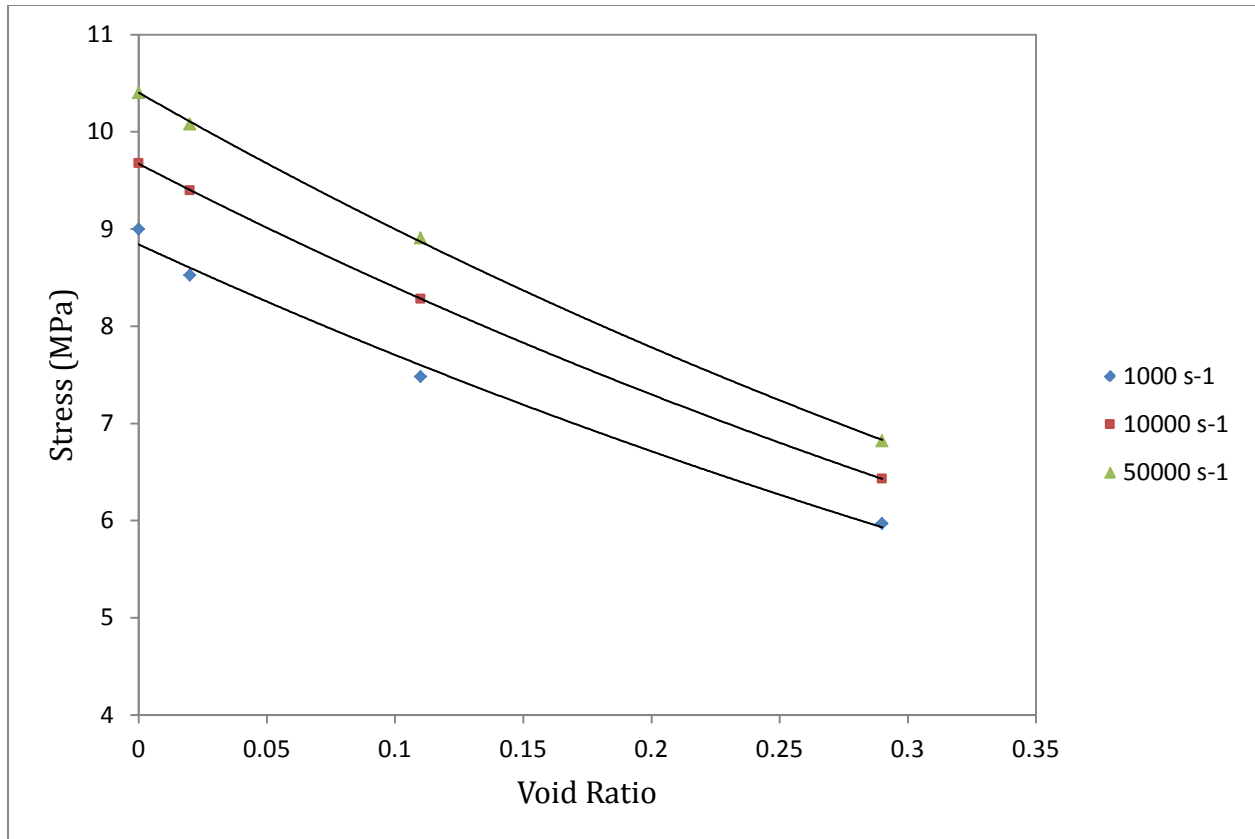


**Fig. 13** Stress vs. void ratio of NPRP at strain 0.05

## 5. CONCLUSION

This study focused on correlation of micro/nano structure morphology to performance of nano enhanced polymers subjected to blast loading, on studying the behavior of the materials at high strain rates, and on evaluation of the effect of the voids on the strain rate sensitivity of these materials. Three polyurea-based elastomeric materials are investigated in this research: unreinforced polyurea; Exfoliated Graphene Nano Particle (xGnP) reinforced polyurea; and Polyhedral Oligomeric Silsesquioxane (POSS) reinforced polyurea. In order to gain insight into the failure mechanism, 3-D CT scans of these materials were conducted, which showed large numbers of voids randomly distributed within materials. Findings show that POSS reinforced polyurea has the largest number and the smallest sized voids among the three tested materials.

Three dimensional finite element (FE) simulations were performed in order to develop an understanding for the voids effect and the strain rate sensitivity of nano particle reinforced polymers. Two methods were used: real volume element and representative volume element. The results of the first method show that the stress was localized and was not distributed uniformly when the voids inside the material have random size and shape. Computational parametric evaluation showed that the mechanical behavior is dependent on strain rate. It also showed that the rate dependence mechanism depends on the void ratio and size, where the stress decreases with the increasing of void's size and ratio inside the specimen when subjected to high strain rates.

## 6. ACKNOWLEDGMENT

The preparation of the XGnP reinforced polyurea and the consultation on material properties provided by Dr. Larry Drzal of Michigan State University and XG Sciences is deeply appreciated. The preparation of POSS reinforced polyurea and consultation provided by Drs. Joe Lichtenhan and Bruce Fu of Hybrid Plastics is also gratefully acknowledged.

This work was partially supported by the funding received under a subcontract from the Department of Homeland Security-Sponsored Southeast Region Research Initiative (SERRI) at the Department of Energy's Oak Ridge National Laboratory, USA.

## REFERENCES

[1] Cheng A., Al-Ostaz A., Raju Mantena P., and Mullen C. (2009). Final report submitted to SERRI. (Available at <http://www.serri.org/publications/Pages/Reports.aspx>).

- [2] Irshidat M., Al-Ostaz A., and Cheng A.H.-D. “Nano-particle reinforced polymer for blast protection of unreinforced masonry wall: laboratory blast load simulation and design models.” *J. Structural Engineering*, in Press.
- [3] Sarva S.S., Deschanel S., Boyce M., and Chen W. (2007). “Stress-strain behavior of a polyurea and a polyurethane from low to high strain rates.” *Polymer*, 48, 2208-2213.
- [4] Amirkhizi A.V., Isaacs J., Mcgee J., and Nemat-Nasser S. (2006). “An Experimentally-based Viscoelastic Constitutive Model for Polyurea, Including Pressure and Temperature Effects,” *Philos Mag.*, 86, 5847-5866.
- [5] Yi J., Boyce M.C., Lee G.F., and Balizer E. (2006). “Large Deformation Rate-Dependent Stress-Strain Behavior of Polyurea and Polyurethane” *Polymer*, 47, 319-329.
- [6] Li C. and Lua J. (2009) “A hyper-viscoelastic constitutive model for polyurea.” *Materials Letters*, 63, 877-880.
- [7] Uddin M. F., Mahfuz H., Zainuddin S., and Jeelani S. (2009) “Improving Ballistic Performance of Polyurethane Foam by Nanoparticle Reinforcement.” *Journal of Nanotechnology*, Vol.2009.
- [8] Lichtenhan J. D., Schwab J. J., and Reinerth W. A. (2001). *Chemical Innovation*, 3-5.  
(<http://pubs.org/subscribe/journals/ci/31/special/0101lead.htm>)